Research Article

Received: 11 December, 2025
Accepted: 03 May, 2026
Published: 17 May, 2026

Kernel-Weighted Vertex Certificates for Modified (h, m)–Convex Functions with Multivariate and Matrix-Valued Applications

Muhammad Ajmal
Department of Mathematics, University of Lahore, Lahore 54000, Pakistan; majmalkhan82@gmail.com

Muhammad Rafaqat
Department of Mathematics, University of Lahore, Lahore 54000, Pakistan

Cite this article:

Ajmal, M., & Rafaqat, M. (2026). Kernel-Weighted Vertex Certificates for Modified (h, m)–Convex Functions with Multivariate and Matrix-Valued Applications. Cultura Científica, (24), pp. 405–431.

Abstract

This paper develops a kernel-weighted framework of explicit vertex certificates for functions satisfying modified (h, m)–convexity of the second type. Motivated by Hermite–Hadamard and Hermite–Hadamard–Fejér type integral bounds, the theory yields computable one-dimensional estimates with kernel expectations, dimension-explicit vertex certificates on rectangular domains through tensorized operators, and radial bounds on origin-anchored simplices via cone decompositions. Matrix counterparts are also obtained, including rigorous trace inequalities in the commuting regime and a conditional extension to noncommuting matrices under an operator-compatibility hypothesis. A central feature of the framework is that the associated kernel coefficients are explicit, one-dimensional, and reusable, so the resulting certificates can be verified directly in practice. Numerical investigations and illustrative computational examples show how the generalized parameters influence the admissible function class, the averaging geometry, and the conservatism of the resulting bounds. These examples also highlight the relevance of the framework to multivariate and matrix-valued applications that require conservative and numerically checkable certificates for integral averages.

Keywords: modified (h, m)–convexity, vertex certificates, computable certificates, kernel-weighted integral operators, multivariate integral bounds, commuting trace inequalities, matrix-valued applications

1. INTRODUCTION

Integral inequalities of Hermite–Hadamard (HH) and Hermite–Hadamard–Fejér (HH–F) type are classical tools for estimating integral means of convex functions under weak smoothness assumptions. For a convex function $f : [a, b] \to \mathbb{R}$, the classical Hermite–Hadamard inequality states that

$$f\left(\frac{a+b}{2}\right) \leq \frac{1}{b-a}\int_a^b f(x)\,dx \leq \frac{f(a)+f(b)}{2}. \tag{1}$$

Such inequalities are fundamental in approximation theory, numerical quadrature, and convex analysis because they relate integral averages to function values at easily computable representative points [1, 2, 3]. A weighted extension due to Fejér takes the form

$$f\left(\frac{a+b}{2}\right) \leq \frac{\int_a^b f(x)w(x)\,dx}{\int_a^b w(x)\,dx} \leq \frac{f(a)+f(b)}{2}, \tag{2}$$

for suitable nonnegative symmetric weights w. In computational settings, such bounds are useful as conservative certificates for average losses, integral objectives, and quadrature validation targets [2, 3, 4].

In higher dimensions, HH-type estimates can serve as tractable surrogates for integral quantities that are expensive to evaluate exactly [2, 5, 6, 7]. Classical multivariate extensions are often built from joint convexity on convex bodies, while an alternative approach uses coordinate-wise convexity on rectangles together with iterated one-dimensional bounds and Fubini-type decompositions [8, 9]. This second viewpoint is especially attractive for computation because it leads to explicit box certificates assembled from lower-dimensional information [10, 11].

A complementary line of work replaces classical convexity by generalized convexity assumptions. Among the most flexible models are (h, m)-type formulations and their modifications, where a control function h and a mixing parameter m describe the underlying geometry [1, 12, 13]. A typical modified (h, m)–convexity condition takes the form

$$f\big(\gamma x + m(1-\gamma)y\big) \leq h(\gamma)^s f(x) + m\big(1-h(\gamma)\big)^s f(y), \qquad \gamma \in [0,1], \tag{3}$$

which reduces to classical convexity when $h(t) = t$, $m = 1$, and $s = 1$. These generalized formulations enlarge the admissible function class while retaining explicit coefficient structure, and recent works have shown that they support HH–F type inequalities beyond the classical convex setting [6, 7, 12].

A further refinement replaces Lebesgue averages by kernel-weighted or fractional-type averages induced by monotone coordinate maps. Such operators are natural when nonuniform sampling, graded meshes, or anisotropic averaging mechanisms are relevant [14]. In the present setting, these operators take the schematic form

$$\mathcal{I}_{\alpha,w}[f] = \int_0^1 f(\xi(t))\,\kappa_\alpha(t)\,dt, \tag{4}$$

where κ_α is a normalized Fejér-symmetric kernel and ξ is the pullback induced by the weight map w. This representation is computationally appealing because the associated coefficients are one-dimensional and can be precomputed and reused across related instances.

HH-type inequalities also appear naturally in matrix analysis and operator theory, where convexity methods lead to trace inequalities, eigenvalue bounds, and certificates for matrix-valued quantities such as quadratic energies and logarithmic determinant barriers [15, 16, 17]. In this setting, however, generalized convexity is substantially more delicate, especially outside the commuting regime, where additional compatibility assumptions become necessary [7, 15, 18, 19].

Against this background, the present paper is best viewed as a theoretical inequality paper with an explicit computational output. Our aim is to develop a unified kernel-weighted HH–F framework that produces computable certificate formulas in one dimension, on multivariate boxes and simplices, and in matrix-valued settings. The paper does not claim a complete application-specific workflow; rather, it provides analytically grounded certificates together with numerical illustrations showing how the generalized parameters affect the strength and interpretation of the resulting bounds.

The main contributions of the paper are as follows:

- We prove a one-dimensional kernel-weighted Hermite–Hadamard–Fejér inequality for functions satisfying modified (h, m)–convexity of the second type, with coefficients expressed as explicit kernel expectations.
- By tensorizing the one-dimensional operator and using coordinate-wise arguments, we derive multivariate box bounds that provide dimension-explicit vertex certificates for integral averages.
- On origin-anchored simplices, we obtain radial HH-type inequalities by combining the generalized convexity assumption with a cone decomposition of the domain.

- In the matrix setting, we establish rigorous commuting-matrix Loewner, trace, and eigenvalue inequalities, together with a conditional noncommuting trace extension under an explicit operator-compatibility hypothesis.

The framework contains several classical inequalities as special cases. If $m = 1$, $s = 1$, $h(t) = t$, each w_i is the identity map, and $\alpha_i = 1$ for all coordinates, then the kernel operator reduces to the usual Lebesgue average

$$\frac{1}{\mathrm{vol}(\mathcal{B})} \int_{\mathcal{B}} f(\mathbf{x})\, d\mathbf{x},$$

and the multivariate results recover the classical Hermite–Hadamard inequalities on rectangles [8, 9, 11]. Likewise, the one-dimensional theory recovers the classical HH–F inequality when $\alpha = 1$.

The paper is organized as follows. Section 2 introduces the generalized convexity assumptions, kernel-weighted operators, and the geometric and operator-theoretic notation used later. Section 3 develops the one-dimensional HH–F bound. Section 4 establishes the tensorized box certificate, and Section 5 derives the radial simplex extension. Section 6 presents the matrix-valued theory, distinguishing the fully rigorous commuting regime from the conditional noncommuting extension. Section 7 contains numerical illustrations and certificate validation, while Section 8 highlights the practical role of the generalized parameters through concrete examples beyond classical convexity. Section 9 discusses implications for optimization and computational workflows, Section 10 summarizes the main limitations, and Section 11 concludes the paper.

2. PRELIMINARIES

This section collects the notation, assumptions, and auxiliary results used throughout the paper. We first recall the generalized convexity framework adopted in the sequel, then introduce the kernel-weighted integral operators that serve as the averaging mechanism in the Hermite–Hadamard–Fejér inequalities, and finally summarize the geometric and operator-theoretic tools required for the multivariate and matrix extensions.

We begin by fixing the notation and geometric settings used throughout the paper.

Let $\mathbb{R}^n$ denote the n-dimensional Euclidean space. For vectors $x = (x_1, \ldots, x_n) \in \mathbb{R}^n$, we write $x \geq 0$ if $x_i \geq 0$ for all i, and $\langle \cdot, \cdot \rangle$ denotes the standard inner product. Throughout the paper, $I = [0, b] \subset \mathbb{R}$ denotes a compact interval with $b > 0$.

For multivariate domains, we consider the origin-anchored box

$$\mathcal{B}(\mathbf{b}) = \prod_{i=1}^{n} [0, b_i], \qquad \mathbf{b} = (b_1, \ldots, b_n) \in (0, \infty)^n,$$

and the origin-anchored simplex

$$\Delta = \mathrm{conv}\{0, v_1, \ldots, v_n\} \subset \mathbb{R}^n,$$

where $0, v_1, \ldots, v_n$ are affinely independent points in $\mathbb{R}^n$. The facet opposite the origin is denoted by

$$\mathcal{F} = \mathrm{conv}\{v_1, \ldots, v_n\}.$$

These two classes of domains provide the natural settings for the coordinate-wise and radial extensions developed later in the paper.

We now recall the generalized convexity notion underlying the present work.

Definition 2.1 (Modified (h, m)–convexity of the second type)**.** Let $m \in (0, 1]$, $s \in [-1, 1]$, and let $h : [0, 1] \to [0, 1]$ be a measurable function with $h \not\equiv 0$. A function $f : [0, b] \to \mathbb{R}$ is said to be *modified (h, m)–convex of the second type with parameter s* if, for all $x, y \in [0, b]$ and $\gamma \in [0, 1]$,

$$f\big(\gamma x + m(1 - \gamma)y\big) \leq h(\gamma)^s f(x) + m\big(1 - h(\gamma)\big)^s f(y).$$

Remark 2.2. Classical convexity is recovered from Definition 2.1 by taking $m = 1$, $h(\gamma) = \gamma$, and $s = 1$. The parameters (h, m, s) therefore quantify how the curvature contribution is distributed between the two endpoints. When $s < 0$, the factors $h(\gamma)^s$ and $\big(1 - h(\gamma)\big)^s$ may become singular near $\gamma = 0$ and $\gamma = 1$. Additional boundedness assumptions are therefore required to ensure the integrability of the kernel coefficients introduced later.

The one-dimensional notion extends naturally to multivariate domains through coordinate-wise and radial formulations. We record both versions here, as each will be used in a different geometric setting.

Definition 2.3 (Coordinate-wise modified (h,m)–convexity)**.** A function $f : \mathcal{B}(\mathbf{b}) \to \mathbb{R}$ is called *coordinate-wise modified (h,m)–convex of the second type with parameter s* if, for each coordinate $i \in \{1,\dots,n\}$ and every fixed choice of the remaining variables, the one-dimensional slice

$$t \mapsto f(x_1,\dots,x_{i-1},t,x_{i+1},\dots,x_n), \qquad t \in [0,b_i],$$

satisfies Definition 2.1.

Definition 2.4 (Radial modified (h,m)–convexity)**.** Let $\Delta = \operatorname{conv}\{0,v_1,\dots,v_n\}$ be an origin-anchored simplex. A function $f : \Delta \to \mathbb{R}$ is said to be *radially modified (h,m)–convex of the second type with parameter s* if, for every $y \in \mathcal{F}$, the function

$$\tau \mapsto f(\tau y), \qquad \tau \in [0,1],$$

satisfies Definition 2.1 along the ray connecting 0 and y.

Remark 2.5. The radial formulation reflects the conic structure of Δ and requires the convexity condition only along rays emanating from the distinguished vertex 0. This structure will later enable a reduction of simplex integrals to one-dimensional radial averages.

To ensure that the kernel expressions introduced below are well defined, we impose the following standing admissibility conditions on the parameters.

Assumption 2.6 (Admissible parameters)**.** Throughout the paper, we fix $m \in (0,1]$ and $s \in [-1,1]$, and assume that $h : [0,1] \to [0,1]$ is measurable with $h \not\equiv 0$. When $s < 0$, we additionally assume that there exists $\eta \in (0,1/2)$ such that

$$h(t) \geq \eta, \qquad 1 - h(t) \geq \eta,$$

for almost every $t \in (0,1)$. This guarantees that the weights $h(t)^s$ and $\big(1-h(t)\big)^s$ remain integrable with respect to the kernel densities introduced below.

We next introduce the averaging operators used throughout the paper. These operators are generated by monotone coordinate maps and symmetric Beta-type kernels, and they form the analytical core of the Hermite–Hadamard–Fejér framework developed in the subsequent sections.

Definition 2.7 (Admissible weight map)**.** Let $b > 0$. A function $w : [0,b] \to \mathbb{R}$ is called *admissible* if it is continuously differentiable, strictly increasing, and satisfies $w'(x) > 0$ for almost every $x \in [0,b]$. In particular, w is invertible on $[0,b]$.

For an admissible weight map w, define the normalized coordinate transformations

$$\theta(x) = \frac{w(x)-w(0)}{w(b)-w(0)} \in [0,1], \qquad \xi(t) = w^{-1}\big(w(0)+t\big(w(b)-w(0)\big)\big), \qquad t \in [0,1]. \tag{5}$$

These maps satisfy $\theta(\xi(t)) = t$ and $\xi(\theta(x)) = x$ for all $x \in [0,b]$.

Definition 2.8 (Fejér-symmetric Beta-type kernel)**.** For $\alpha > 0$, define

$$\kappa_\alpha(t) = \frac{\alpha}{2}\left(t^{\alpha-1} + (1-t)^{\alpha-1}\right), \qquad t \in (0,1). \tag{6}$$

Then $\kappa_\alpha(t) = \kappa_\alpha(1-t)$, $\kappa_\alpha(t) \geq 0$, and

$$\int_0^1 \kappa_\alpha(t)\,dt = 1.$$

Hence, κ_α defines a probability density on $(0,1)$. When $\alpha \in (0,1)$, the kernel has integrable endpoint singularities, whereas for $\alpha \geq 1$ it is bounded.

Throughout the paper, vectors are written in boldface, coordinate indices run over $i = 1,\dots,n$, and all integrals are understood in the Lebesgue sense unless stated otherwise. The symbols $H_\alpha(h,s)$ and $\widetilde{H}_\alpha(h,s)$ denote the kernel expectations defined below.

We now formalize the one-dimensional weighted averaging operator that will later be tensorized and adapted to more general settings.

Definition 2.9 (Two-sided normalized w-kernel operator)**.** For $\alpha > 0$ and an admissible weight map $w : [0, b] \to \mathbb{R}$, define the weighted fractional integrals with respect to w by

$$(I_{0^+}^{\alpha,w} g)(b) := \frac{1}{\Gamma(\alpha)} \int_0^b \big(w(b) - w(t)\big)^{\alpha-1} w'(t) g(t)\, dt, \tag{7}$$

$$(I_{b^-}^{\alpha,w} g)(0) := \frac{1}{\Gamma(\alpha)} \int_0^b \big(w(t) - w(0)\big)^{\alpha-1} w'(t) g(t)\, dt. \tag{8}$$

The associated two-sided normalized operator is defined by

$$\mathcal{I}_{\alpha,w}[g; 0, b] := \frac{\Gamma(\alpha+1)}{2\big(w(b) - w(0)\big)^{\alpha}} \left((I_{0^+}^{\alpha,w} g)(b) + (I_{b^-}^{\alpha,w} g)(0) \right). \tag{9}$$

The following lemma establishes the probabilistic representation of $\mathcal{I}_{\alpha,w}$ as a kernel average.

Lemma 2.10 (Kernel normalization identity)**.** *Let $\alpha > 0$ and let w be an admissible weight map. If g is measurable and the following integrals are finite, then*

$$\mathcal{I}_{\alpha,w}[g; 0, b] = \int_0^1 g(\xi(t))\, \kappa_\alpha(t)\, dt, \tag{10}$$

where ξ is defined in (5) *and κ_α is defined in* (6)*. In particular, for bounded measurable g, $\mathcal{I}_{\alpha,w}$ is a positive normalized linear functional.*

Proof. Expand $\mathcal{I}_{\alpha,w}$ using Definition 2.9 and the identity $\Gamma(\alpha+1) = \alpha\Gamma(\alpha)$. Put

$$u = \theta(t) = \frac{w(t) - w(0)}{w(b) - w(0)}.$$

Then $t = \xi(u)$ and

$$w'(t)\, dt = \big(w(b) - w(0)\big)\, du.$$

For the term $(I_{b^-}^{\alpha,w} g)(0)$, this substitution gives the factor $u^{\alpha-1}$. For the term $(I_{0^+}^{\alpha,w} g)(b)$, the same substitution gives the factor $(1-u)^{\alpha-1}$. Combining the two contributions and simplifying yields

$$\mathcal{I}_{\alpha,w}[g; 0, b] = \frac{\alpha}{2} \int_0^1 g(\xi(u)) \left(u^{\alpha-1} + (1-u)^{\alpha-1} \right) du,$$

which is exactly (10). The normalization of κ_α follows by direct integration of (6). □

Remark 2.11. The representation (10) is fundamental for the multivariate extension. It shows that $\mathcal{I}_{\alpha,w}$ averages the function g along the w-affine path connecting the endpoints with a symmetric two-sided weight. This symmetry is essential for stable tensorization in higher dimensions, mirroring the role of Fejér weights in classical HH–F theory [6, 17, 20].

The constants that appear throughout the multivariate bounds are one-dimensional kernel expectations derived from the generalized convexity parameters. We record them next for later reference.

Definition 2.12 (Kernel coefficients)**.** For $\alpha > 0$, define

$$H_\alpha(h, s) := \int_0^1 h(t)^s \kappa_\alpha(t)\, dt, \qquad \widetilde{H}_\alpha(h, s) := \int_0^1 \big(1 - h(t)\big)^s \kappa_\alpha(t)\, dt. \tag{11}$$

Under Assumption 2.6, these integrals are finite and yield nonnegative coefficients. For the canonical choice $h(t) = t$, they reduce to expressions involving the Beta function:

$$H_\alpha(\mathrm{id}, s) = \frac{\alpha}{2} \left(\frac{1}{\alpha + s} + \mathrm{B}(s+1, \alpha) \right), \qquad \widetilde{H}_\alpha(\mathrm{id}, s) = \frac{\alpha}{2} \left(\frac{1}{\alpha + s} + \mathrm{B}(\alpha, s+1) \right), \tag{12}$$

where $\mathrm{B}(\cdot, \cdot)$ denotes the Beta function. These expressions are finite whenever $s > -1$ and $\alpha + s > 0$.

The one-dimensional operator above admits a natural product extension on boxes, which will be used to derive dimension-explicit estimates in later sections.

Definition 2.13 (Tensorized kernel operator on a box)**.** For each coordinate $i \in \{1, \dots, n\}$, fix $\alpha_i > 0$ and an admissible weight map $w_i : [0, b_i] \to \mathbb{R}$. Define the coordinate pullbacks $\xi_i : [0, 1] \to [0, b_i]$ by (5), with w replaced by w_i. For an integrable function $f : \mathcal{B}(\mathbf{b}) \to \mathbb{R}$, define

$$\mathcal{I}_{\boldsymbol{\alpha},\mathbf{w}}[f; \mathcal{B}(\mathbf{b})] := \int_{[0,1]^n} f\big(\xi_1(t_1), \dots, \xi_n(t_n)\big) \prod_{i=1}^{n} \kappa_{\alpha_i}(t_i)\, d\mathbf{t}. \tag{13}$$

By Fubini's theorem and Lemma 2.10, this operator coincides with the iterated application of the one-dimensional operators along each coordinate. This product structure is exploited in Theorem 4.1 to obtain dimension-explicit vertex bounds.

We conclude this preliminary part with the geometric identity that underlies the simplex-based formulation.

Lemma 2.14 (Cone decomposition of simplex integrals)**.** *Let $\Delta = \operatorname{conv}\{0, v_1, \dots, v_n\} \subset \mathbb{R}^n$ be a nondegenerate simplex, and let*

$$\mathcal{F} = \operatorname{conv}\{v_1, \dots, v_n\}$$

be its facet opposite the origin. Equip $\mathcal{F}$ with the induced $(n-1)$-dimensional Hausdorff measure $d\sigma$. Then, for any $g \in L^1(\Delta)$,

$$\int_\Delta g(x)\, dx = \frac{n \operatorname{vol}(\Delta)}{\sigma(\mathcal{F})} \int_0^1 \int_{\mathcal{F}} g(\tau y)\, \tau^{n-1}\, d\sigma(y)\, d\tau. \tag{14}$$

Equivalently, if $d\mu_{\mathcal{F}} = d\sigma/\sigma(\mathcal{F})$ is the normalized surface measure on $\mathcal{F}$, then

$$\frac{1}{\operatorname{vol}(\Delta)} \int_\Delta g(x)\, dx = n \int_0^1 \int_{\mathcal{F}} g(\tau y)\, \tau^{n-1}\, d\mu_{\mathcal{F}}(y)\, d\tau. \tag{15}$$

Proof. Consider the map $T : [0, 1] \times \mathcal{F} \to \Delta$ defined by $T(\tau, y) = \tau y$. Restricted to $(0, 1) \times \mathcal{F}$, this map parametrizes $\Delta \setminus \{0\}$. Scaling by τ multiplies the tangential $(n-1)$-dimensional measure on $\mathcal{F}$ by τ^{n-1}. The remaining constant is determined by applying the formula to $g \equiv 1$, which gives the normalization factor

$$\frac{n \operatorname{vol}(\Delta)}{\sigma(\mathcal{F})}.$$

Substituting this factor into the change-of-variables formula gives (14). Dividing both sides by $\operatorname{vol}(\Delta)$ yields (15). □

Remark 2.15. This decomposition is the key to reducing simplex integrals to one-dimensional radial averages, which will be combined with radial modified convexity in Section 5.

3. ONE-DIMENSIONAL HH–F BOUND UNDER MODIFIED (h, m)–CONVEXITY

This section establishes the one-dimensional kernel-weighted Hermite–Hadamard–Fejér inequality that serves as the base case for the multivariate theory developed later. The result is formulated so that the constants are explicit, the admissibility requirements are transparent, and the proof reduces the estimate to the defining modified (h, m)–convexity condition integrated against a normalized Fejér-symmetric kernel.

Let $b > 0$ and let $w : [0, b] \to \mathbb{R}$ be an admissible weight map in the sense of Definition 2.7. Denote the normalized w-coordinate by

$$\theta(x) := \frac{w(x) - w(0)}{w(b) - w(0)} \in [0, 1], \qquad \xi(t) := w^{-1}\big(w(0) + t\big(w(b) - w(0)\big)\big), \qquad t \in [0, 1]. \tag{16}$$

Then $\theta(\xi(t)) = t$ for all $t \in [0, 1]$, and $\xi(\theta(x)) = x$ for all $x \in [0, b]$.

For $\alpha > 0$, recall the Fejér-symmetric Beta-type kernel

$$\kappa_\alpha(t) := \frac{\alpha}{2}\left(t^{\alpha-1} + (1-t)^{\alpha-1}\right), \qquad t \in (0, 1), \tag{17}$$

which satisfies $\kappa_\alpha(t) \geq 0$ and

$$\int_0^1 \kappa_\alpha(t)\, dt = 1.$$

By Lemma 2.10, the two-sided normalized weighted operator admits the representation

$$\mathcal{I}_{\alpha,w}[g; 0, b] = \int_0^1 g(\xi(t))\, \kappa_\alpha(t)\, dt, \tag{18}$$

whenever the integral is finite.

For a general admissible weight map w, define the w-dependent kernel coefficients by

$$H_{\alpha,w}^{(b)}(h,s) := \int_0^1 h\left(\frac{\xi(t)}{b}\right)^s \kappa_\alpha(t)\,dt, \qquad \widetilde{H}_{\alpha,w}^{(b)}(h,s) := \int_0^1 \left(1-h\left(\frac{\xi(t)}{b}\right)\right)^s \kappa_\alpha(t)\,dt. \tag{19}$$

Under Assumption 2.6, these coefficients are finite and nonnegative. If w is affine, then $\xi(t) = bt$, and the coefficients reduce to

$$H_{\alpha,w}^{(b)}(h,s) = H_\alpha(h,s), \qquad \widetilde{H}_{\alpha,w}^{(b)}(h,s) = \widetilde{H}_\alpha(h,s).$$

Theorem 3.1 (One-dimensional kernel-weighted HH–F upper bound)**.** *Assume Assumption 2.6, and let w be an admissible weight map on $[0,b]$. Let $f:[0,b]\to\mathbb{R}$ be measurable and integrable, and suppose that f is modified (h,m)–convex of the second type with parameter s on $[0,b]$ in the sense of Definition 2.1. Then, for every $\alpha>0$,*

$$\mathcal{I}_{\alpha,w}[f;0,b] \le H_{\alpha,w}^{(b)}(h,s)f(b) + m\,\widetilde{H}_{\alpha,w}^{(b)}(h,s)f(0). \tag{20}$$

Moreover, equality holds in (20) *whenever*

$$f(\xi(t)) = h\left(\frac{\xi(t)}{b}\right)^s f(b) + m\left(1-h\left(\frac{\xi(t)}{b}\right)\right)^s f(0)$$

for κ_α-almost every $t\in(0,1)$.

Proof. By Definition 2.1, for all $x,y\in[0,b]$ and all $\gamma\in[0,1]$,

$$f\big(\gamma x + m(1-\gamma)y\big) \le h(\gamma)^s f(x) + m\big(1-h(\gamma)\big)^s f(y). \tag{21}$$

Choose $x=b$, $y=0$, and

$$\gamma = \frac{\xi(t)}{b}.$$

Since $\xi(t)\in[0,b]$, we have $\gamma\in[0,1]$. Therefore,

$$f(\xi(t)) = f\left(\frac{\xi(t)}{b}b + m\left(1-\frac{\xi(t)}{b}\right)0\right) \le h\left(\frac{\xi(t)}{b}\right)^s f(b) + m\left(1-h\left(\frac{\xi(t)}{b}\right)\right)^s f(0).$$

Multiplying this inequality by $\kappa_\alpha(t)\ge 0$ and integrating over $(0,1)$ gives

$$\begin{aligned}\int_0^1 f(\xi(t))\kappa_\alpha(t)\,dt \le &\left[\int_0^1 h\left(\frac{\xi(t)}{b}\right)^s \kappa_\alpha(t)\,dt\right] f(b)\\ &+ m\left[\int_0^1 \left(1-h\left(\frac{\xi(t)}{b}\right)\right)^s \kappa_\alpha(t)\,dt\right] f(0).\end{aligned}$$

Using (18) and (19), we obtain (20). □

Remark 3.2 (Normalization of the vertex coefficients). For each coordinate i, the coefficients satisfy

$$c_i(1) + c_i(0) = H_i + m\,\widetilde{H}_i.$$

Consequently, the total weight appearing in (22) satisfies

$$\sum_{\boldsymbol{\varepsilon}\in\{0,1\}^n} C_{\boldsymbol{\varepsilon}} = \prod_{i=1}^n (H_i + m\,\widetilde{H}_i).$$

In the classical specialization $m=1$, $h(t)=t$, $w_i(t)=t$, and $\alpha_i=1$, one has

$$H_i = \widetilde{H}_i = \frac{1}{2},$$

and therefore

$$\sum_{\boldsymbol{\varepsilon}\in\{0,1\}^n} C_{\boldsymbol{\varepsilon}} = 1.$$

Thus, the classical Hadamard bound corresponds to a normalized vertex average.

Remark 3.3 (Fejér-type structure and symmetry). The kernel κ_α in (17) is symmetric under the transformation $t \mapsto 1-t$. Accordingly, $\mathcal{I}_{\alpha,w}$ averages f along the w-affine segment between the endpoints using a genuinely two-sided Fejér-type weight rather than a one-sided fractional bias. This symmetry is essential for the tensorized construction developed in the multivariate setting.

Remark 3.4 (Computability of the constants). The coefficients $H_\alpha(h,s)$ and $\widetilde{H}_\alpha(h,s)$ are explicit kernel expectations and are therefore directly computable once h is specified. For the canonical choice $h(t)=t$, one obtains the Beta-function expressions stated in Definition 2.12. Such closed forms are useful when extracting dimension-dependent constants after tensorization.

Remark 3.5 (Recovery of the classical HH upper bound). If $m=1$, $s=1$, $h(t)=t$, $w(t)=t$, and $\alpha=1$, then $\kappa_1(t)\equiv 1$, and (20) reduces to

$$\frac{1}{b}\int_0^b f(x)\,dx \le \frac{f(0)+f(b)}{2},$$

which is the classical Hermite–Hadamard upper bound.

4. MULTIVARIATE HH–F INEQUALITIES ON BOXES IN $\mathbb{R}^n$

This section develops dimension-explicit Hermite–Hadamard–Fejér (HH–F) bounds on origin-anchored boxes under coordinate-wise modified (h,m)–convexity of the second type. The main result is a vertex-dominated inequality in which the tensorized kernel operator is controlled by a weighted combination of the 2^n vertex values. The bound is fully explicit, since all coefficients factorize coordinate-wise and are directly computable from one-dimensional kernel expectations.

Let

$$\mathcal{B}(\mathbf{b}) = \prod_{i=1}^n [0,b_i], \qquad \mathbf{b}\in(0,\infty)^n,$$

and let

$$v_{\boldsymbol{\varepsilon}} = (\varepsilon_1 b_1,\dots,\varepsilon_n b_n), \qquad \boldsymbol{\varepsilon}\in\{0,1\}^n,$$

denote the vertices of $\mathcal{B}(\mathbf{b})$. For each coordinate i, fix $\alpha_i>0$ and an admissible weight map $w_i:[0,b_i]\to\mathbb{R}$. Recall from Definition 2.12 that

$$H_{\alpha_i}(h,s) = \int_0^1 h(t)^s\,\kappa_{\alpha_i}(t)\,dt, \qquad \widetilde{H}_{\alpha_i}(h,s) = \int_0^1 \big(1-h(t)\big)^s\,\kappa_{\alpha_i}(t)\,dt,$$

where κ_α is the Fejér-symmetric kernel introduced in Definition 2.8. Under Assumption 2.6, these coefficients are finite and nonnegative.

Theorem 4.1 (Kernel-weighted HH–F vertex bound on boxes)**.** *Assume Assumption 2.6. Let $f:\mathcal{B}(\mathbf{b})\to\mathbb{R}$ be measurable and integrable, and suppose that f is coordinate-wise modified (h,m)–convex of the second type with parameter s on $\mathcal{B}(\mathbf{b})$ in the sense of Definition 2.3. Then*

$$\mathcal{I}_{\boldsymbol{\alpha},\mathbf{w}}[f;\mathcal{B}(\mathbf{b})] \le \sum_{\boldsymbol{\varepsilon}\in\{0,1\}^n} C_{\boldsymbol{\varepsilon}}\, f(v_{\boldsymbol{\varepsilon}}), \tag{22}$$

where the vertex weights factorize coordinate-wise as

$$C_{\boldsymbol{\varepsilon}} := \prod_{i=1}^n c_i(\varepsilon_i), \qquad c_i(1) := H_{\alpha_i}(h,s), \qquad c_i(0) := m\,\widetilde{H}_{\alpha_i}(h,s). \tag{23}$$

Proof. By Definition 2.13 and Lemma 2.10, the tensorized operator can be written as

$$\mathcal{I}_{\boldsymbol{\alpha},\mathbf{w}}[f;\mathcal{B}(\mathbf{b})] = \int_{[0,1]^n} f\big(\boldsymbol{\xi}(\mathbf{t})\big)\prod_{i=1}^n \kappa_{\alpha_i}(t_i)\,d\mathbf{t}, \tag{24}$$

where

$$\boldsymbol{\xi}(\mathbf{t}) = \big(\xi_1(t_1),\dots,\xi_n(t_n)\big).$$

By Fubini's theorem, the integral can be evaluated iteratively, one coordinate at a time.

Fix

$$\mathbf{t}' = (t_1,\dots,t_{n-1}) \in [0,1]^{n-1}$$

and define the slice

$$g_{\mathbf{t}'}(x_n) := f\big(\xi_1(t_1), \dots, \xi_{n-1}(t_{n-1}), x_n\big), \qquad x_n \in [0, b_n].$$

Since f is coordinate-wise modified (h, m)–convex, the function $g_{\mathbf{t}'}$ is modified (h, m)–convex of the second type on $[0, b_n]$. Applying Theorem 3.1 to $g_{\mathbf{t}'}$ gives

$$\begin{aligned}
&\int_0^1 f\big(\boldsymbol{\xi}'(\mathbf{t}'), \xi_n(t_n)\big)\kappa_{\alpha_n}(t_n)\, dt_n \\
&\quad = \int_0^1 g_{\mathbf{t}'}\big(\xi_n(t_n)\big)\kappa_{\alpha_n}(t_n)\, dt_n \\
&\quad \le H_{\alpha_n}(h, s)\, g_{\mathbf{t}'}(b_n) + m\, \widetilde{H}_{\alpha_n}(h, s)\, g_{\mathbf{t}'}(0) \\
&\quad = H_{\alpha_n}(h, s)\, f\big(\boldsymbol{\xi}'(\mathbf{t}'), b_n\big) + m\, \widetilde{H}_{\alpha_n}(h, s)\, f\big(\boldsymbol{\xi}'(\mathbf{t}'), 0\big),
\end{aligned} \tag{25}$$

where

$$\boldsymbol{\xi}'(\mathbf{t}') = \big(\xi_1(t_1), \dots, \xi_{n-1}(t_{n-1})\big).$$

Substituting (25) into (24) yields

$$\begin{aligned}
\mathcal{I}_{\boldsymbol{\alpha},\mathbf{w}}[f; \mathcal{B}(\mathbf{b})] \le H_{\alpha_n}(h, s) \int_{[0,1]^{n-1}} f\big(\boldsymbol{\xi}'(\mathbf{t}'), b_n\big) \prod_{i=1}^{n-1} \kappa_{\alpha_i}(t_i)\, d\mathbf{t}' \\
+ m\, \widetilde{H}_{\alpha_n}(h, s) \int_{[0,1]^{n-1}} f\big(\boldsymbol{\xi}'(\mathbf{t}'), 0\big) \prod_{i=1}^{n-1} \kappa_{\alpha_i}(t_i)\, d\mathbf{t}'.
\end{aligned} \tag{26}$$

Now define

$$f^{(1)}(\mathbf{x}') := f(\mathbf{x}', b_n), \qquad f^{(0)}(\mathbf{x}') := f(\mathbf{x}', 0),$$

on the $(n-1)$-dimensional face

$$\prod_{i=1}^{n-1} [0, b_i].$$

Both functions inherit coordinate-wise modified (h, m)–convexity from f by restriction. Repeating the same argument recursively over the coordinates $n-1, n-2, \dots, 1$, one obtains a sum over all vertices of $\mathcal{B}(\mathbf{b})$, where each coordinate contributes either the factor $H_{\alpha_i}(h, s)$ when the endpoint b_i is selected or the factor $m\, \widetilde{H}_{\alpha_i}(h, s)$ when the endpoint 0 is selected. This yields (22) with coefficients given by (23). □

Remark 4.2 (Structural meaning of the coefficients). Theorem 4.1 is dimension-explicit in a strong sense. The multivariate constant is not a single aggregated quantity, but rather a family of vertex weights

$$\{C_{\boldsymbol{\varepsilon}}\}_{\boldsymbol{\varepsilon} \in \{0,1\}^n}$$

that factorizes into one-dimensional kernel expectations. Once h, s, m, and the pairs (α_i, w_i) are fixed, all coefficients can be computed independently by one-dimensional quadrature.

Remark 4.3 (Tightness mechanism). The proof shows that equality in (22) holds whenever the one-dimensional inequality from Theorem 3.1 is saturated on almost every slice in every coordinate. In this sense, extremizers arise from iterated saturation of the one-dimensional modified (h, m)–convex interpolation along the coordinate-wise w_i-affine paths.

Remark 4.4 (Vertex certificates and scalability). The right-hand side of (22) gives a vertex certificate that bounds the tensorized integral average using at most 2^n function evaluations. This certificate is exact within the current framework, although it may be expensive to evaluate when n is large. However, the tensor-product structure suggests possible relaxations, for example by grouping coordinates or replacing the full vertex certificate with lower-dimensional face certificates.

The preceding theorem recovers the standard Hadamard-type bound on boxes as a limiting case.

Corollary 4.5 (Classical coordinate-wise convexity bound as a limiting case)**.** *Let $m = 1$, $s = 1$, $h(t) = t$, and suppose that $w_i(t) = t$ and $\alpha_i = 1$ for all $i = 1, \dots, n$. If f is coordinate-wise convex on $\mathcal{B}(\mathbf{b})$ in the classical sense, then*

$$\frac{1}{\operatorname{vol}(\mathcal{B}(\mathbf{b}))} \int_{\mathcal{B}(\mathbf{b})} f(\mathbf{x})\, d\mathbf{x} \le \frac{1}{2^n} \sum_{\boldsymbol{\varepsilon} \in \{0,1\}^n} f(v_{\boldsymbol{\varepsilon}}). \tag{27}$$

For $n = 2$, (27) *reduces to the familiar Hadamard-type inequality on rectangles for coordinate-wise convex functions.*

Proof. Under the stated specialization, $\kappa_1(t) \equiv 1$, and Definition 2.13 becomes the uniform average over $\mathcal{B}(\mathbf{b})$:

$$\mathcal{I}_{\boldsymbol{\alpha},\mathbf{w}}[f;\mathcal{B}(\mathbf{b})] = \frac{1}{\mathrm{vol}(\mathcal{B}(\mathbf{b}))}\int_{\mathcal{B}(\mathbf{b})} f(\mathbf{x})\,d\mathbf{x}.$$

Moreover,

$$H_1(\mathrm{id},1) = \int_0^1 t\,dt = \frac{1}{2}, \qquad \widetilde{H}_1(\mathrm{id},1) = \int_0^1 (1-t)\,dt = \frac{1}{2}.$$

Thus $c_i(0) = c_i(1) = 1/2$ for every coordinate. Hence

$$C_{\boldsymbol{\varepsilon}} = \prod_{i=1}^{n} \frac{1}{2} = 2^{-n},$$

and Theorem 4.1 immediately yields (27). □

5. RADIAL HH-TYPE BOUNDS ON SIMPLICES

Unlike boxes, simplices do not admit a coordinate-wise product structure. Nevertheless, an origin-anchored simplex

$$\Delta = \mathrm{conv}\{0, v_1, \dots, v_n\}$$

has a canonical cone parametrization from the distinguished vertex 0. This reduces volume integration over Δ to an iterated integral over the opposite facet and a one-dimensional radial variable, which in turn makes it possible to derive HH-type estimates under radial modified (h,m)–convexity. The resulting bounds are dimension-explicit and retain transparent dependence on the generalized convexity parameters.

We now use the cone decomposition from Lemma 2.14 to derive a simplex analogue of the HH upper bound. Since Δ does not tensorize, the natural comparison involves the facet average and the distinguished vertex value $f(0)$.

Theorem 5.1 (Simplex HH-type upper bound for radial modified (h,m)–convexity)**.** *Assume Assumption 2.6. Let*

$$\Delta = \mathrm{conv}\{0, v_1, \dots, v_n\}$$

be a nondegenerate simplex, and let

$$\mathcal{F} = \mathrm{conv}\{v_1, \dots, v_n\}$$

be its facet opposite the origin. Let $f : \Delta \to \mathbb{R}$ be measurable and integrable, and suppose that f is radially modified (h,m)–convex of the second type with parameter s in the sense of Definition 2.4. Then

$$\frac{1}{\mathrm{vol}(\Delta)}\int_\Delta f(x)\,dx \le A_n(h,s)\,\frac{1}{\sigma(\mathcal{F})}\int_{\mathcal{F}} f(y)\,d\sigma(y) + m\,B_n(h,s)\,f(0), \tag{28}$$

where

$$A_n(h,s) := n\int_0^1 h(\tau)^s\,\tau^{n-1}\,d\tau, \qquad B_n(h,s) := n\int_0^1 \big(1-h(\tau)\big)^s\,\tau^{n-1}\,d\tau. \tag{29}$$

Proof. Fix $y \in \mathcal{F}$. By radial modified (h,m)–convexity, the function $\tau \mapsto f(\tau y)$ satisfies the one-dimensional inequality

$$f(\tau y) = f\big(\tau y + m(1-\tau)0\big) \le h(\tau)^s f(y) + m\big(1-h(\tau)\big)^s f(0), \qquad \tau \in [0,1]. \tag{30}$$

Multiplying (30) by $\tau^{n-1} \ge 0$ and integrating over $\tau \in [0,1]$, we obtain

$$\begin{aligned}\int_0^1 f(\tau y)\,\tau^{n-1}\,d\tau \le{}& \left(\int_0^1 h(\tau)^s\,\tau^{n-1}\,d\tau\right) f(y)\\ &+ m\left(\int_0^1 \big(1-h(\tau)\big)^s\,\tau^{n-1}\,d\tau\right) f(0).\end{aligned} \tag{31}$$

Let

$$d\mu_{\mathcal{F}}(y) = \frac{d\sigma(y)}{\sigma(\mathcal{F})}$$

be the normalized surface measure on $\mathcal{F}$. By the normalized cone decomposition of simplex integrals,

$$\frac{1}{\mathrm{vol}(\Delta)}\int_\Delta f(x)\,dx = n\int_0^1\int_{\mathcal{F}} f(\tau y)\,\tau^{n-1}\,d\mu_{\mathcal{F}}(y)\,d\tau.$$

Integrating (31) with respect to $d\mu_{\mathcal{F}}(y)$ and multiplying by n gives (28). □

Remark 5.2 (Interpretation of the constants). The coefficients in (28) are normalized radial moments. Indeed, if

$$\rho_n(\tau) = n\,\tau^{n-1}\mathbf{1}_{(0,1)}(\tau),$$

then ρ_n is a probability density on $(0,1)$, and

$$A_n(h,s) = \mathbb{E}_{\rho_n}[h(\tau)^s], \qquad B_n(h,s) = \mathbb{E}_{\rho_n}\big[(1-h(\tau))^s\big].$$

This probabilistic representation makes the dependence on the generalized convexity parameters explicit and facilitates concrete evaluation for standard choices of h.

Remark 5.3 (Classical normalization of the simplex coefficients). In the classical specialization $m = 1$, $s = 1$, and $h(t) = t$, the coefficients in (29) satisfy

$$A_n(t,1) = n\int_0^1 t\,t^{n-1}\,dt = \frac{n}{n+1}, \qquad B_n(t,1) = n\int_0^1 (1-t)t^{n-1}\,dt = \frac{1}{n+1}.$$

Hence $A_n(t,1)+B_n(t,1) = 1$, and inequality (28) reduces to the classical Hermite–Hadamard upper bound on simplices, where the domain average is controlled by a convex combination of the facet average and the value at the distinguished vertex [4, 17, 21, 22].

Remark 5.4 (From facet averages to vertex bounds). If the restriction of f to the facet $\mathcal{F}$ enjoys additional structure, then the facet average in (28) can itself be bounded by finitely many vertex values. For example, if $\mathcal{F}$ is represented in an affine chart where $f|_{\mathcal{F}}$ is coordinate-wise modified (h,m)–convex, then the box inequality from Section 4 can be applied on that chart to produce an explicit pure-vertex certificate involving $\{f(v_i)\}_{i=1}^n$ together with $f(0)$.

6. OPERATOR AND MATRIX EXTENSIONS

We next develop matrix-valued counterparts of the scalar HH–F framework. Since modified (h,m)–convexity involves the nonlinear coefficient functions $h(\gamma)^s$ and $\big(1-h(\gamma)\big)^s$, lifting scalar inequalities to noncommutative settings requires additional care. In contrast with standard convexity, for which operator convexity and Jensen-type inequalities provide a well-established Loewner-order theory, there is no general principle ensuring that the modified (h,m)–convexity inequality is preserved under functional calculus for arbitrary noncommuting matrices [10]. For this reason, we distinguish two regimes:

1. *Commuting regime.* If the matrices commute, simultaneous diagonalization reduces the problem to the scalar setting. This yields fully rigorous Loewner-order, trace, and eigenvalue bounds without additional operator-convexity assumptions.

2. *Noncommuting regime.* For general A, B, one must impose an explicit operator-level compatibility condition, namely a Loewner-order version of modified (h,m)–convexity. Under this assumption, the HH–F trace mechanism extends directly.

Let $\mathbb{H}_d$ denote the real vector space of Hermitian $d \times d$ matrices, and let $\mathbb{H}_d^{++}$ denote the cone of positive definite Hermitian matrices. For $X, Y \in \mathbb{H}_d$, we write $X \preceq Y$ for the Loewner order, meaning that $Y - X$ is positive semidefinite. For a continuous function $\varphi : (0,\infty) \to \mathbb{R}$ and $A \in \mathbb{H}_d^{++}$, the matrix $\varphi(A)$ is defined via functional calculus. We use $\mathrm{tr}(\cdot)$ for the trace and $\lambda_{\max}(\cdot)$ for the largest eigenvalue.

Definition 6.1 (Operator modified (h,m)–convexity)**.** Fix the parameters as in Assumption 2.6. A function $\varphi : (0,\infty) \to \mathbb{R}$ is said to be *operator modified (h,m)–convex of the second type with parameter s* if, for every dimension $d \in \mathbb{N}$, all $A, B \in \mathbb{H}_d^{++}$, and all $\gamma \in [0,1]$,

$$\varphi\big(\gamma A + m(1-\gamma)B\big) \preceq h(\gamma)^s\,\varphi(A) + m\big(1-h(\gamma)\big)^s\,\varphi(B). \tag{32}$$

Remark 6.2 (Why this assumption is stated explicitly). Operator convexity alone does not generally imply (32), because the modified (h,m)–weights are not generated by the standard Jensen coefficients [10]. Definition 6.1 therefore states explicitly the hypothesis needed for a genuine Loewner-order lift of the scalar theory.

The commuting case provides the most robust part of the operator theory developed here.

Proposition 6.3 (Commuting Loewner lift of scalar modified (h,m)–convexity)**.** *Let $\varphi : (0,\infty) \to \mathbb{R}$ satisfy the scalar modified (h,m)–convexity inequality on $(0,\infty)$. If $A, B \in \mathbb{H}_d^{++}$ commute, then, for every $\gamma \in [0,1]$,*

$$\varphi\big(\gamma A + m(1-\gamma)B\big) \preceq h(\gamma)^s\,\varphi(A) + m\big(1-h(\gamma)\big)^s\,\varphi(B). \tag{33}$$

Proof. Since A and B are commuting Hermitian matrices, there exists a unitary matrix U such that

$$A = U\,\mathrm{diag}(a_1,\dots,a_d)U^*, \qquad B = U\,\mathrm{diag}(b_1,\dots,b_d)U^*,$$

with $a_i, b_i > 0$ for all i. Functional calculus gives

$$\varphi\big(\gamma A + m(1-\gamma)B\big) = U\,\mathrm{diag}\left(\varphi\big(\gamma a_i + m(1-\gamma)b_i\big)\right)_{i=1}^{d} U^*,$$

and similarly for $\varphi(A)$ and $\varphi(B)$. Applying the scalar modified (h,m)–convexity inequality componentwise to each pair (a_i, b_i) gives the corresponding diagonal matrix inequality, which is equivalent to the Loewner-order statement (33). □

Theorem 6.4 (Kernel-weighted trace HH–F inequality for commuting matrices)**.** *Assume Assumption 2.6. Let $A, B \in \mathbb{H}_d^{++}$ commute, and let $\varphi : (0,\infty) \to \mathbb{R}$ satisfy scalar modified (h,m)–convexity of the second type with parameter s. Then, for every $\alpha > 0$,*

$$\int_0^1 \mathrm{tr}\big(\varphi\big(tA + m(1-t)B\big)\big)\,\kappa_\alpha(t)\,dt \le H_\alpha(h,s)\ \mathrm{tr}(\varphi(A)) + m\,\widetilde{H}_\alpha(h,s)\ \mathrm{tr}(\varphi(B)). \tag{34}$$

Proof. For each $t \in [0,1]$, Proposition 6.3 gives

$$\varphi\big(tA + m(1-t)B\big) \preceq h(t)^s\,\varphi(A) + m\big(1-h(t)\big)^s\,\varphi(B).$$

Since $\kappa_\alpha(t) \ge 0$ and the trace is monotone on positive semidefinite matrices, multiplying by $\kappa_\alpha(t)$, taking traces, and integrating over $t \in [0,1]$ gives

$$\int_0^1 \mathrm{tr}\big(\varphi\big(tA + m(1-t)B\big)\big)\,\kappa_\alpha(t)\,dt \le \left(\int_0^1 h(t)^s\kappa_\alpha(t)\,dt\right)\mathrm{tr}(\varphi(A)) + m\left(\int_0^1 \big(1-h(t)\big)^s\kappa_\alpha(t)\,dt\right)\mathrm{tr}(\varphi(B)).$$

This is exactly (34). □

Remark 6.5 (Eigenvalue-level variants). Under the same commuting assumptions, the argument also yields componentwise eigenvalue bounds. In particular, if the eigenvalues are ordered consistently under simultaneous diagonalization, then, for each k,

$$\int_0^1 \lambda_k\big(\varphi\big(tA + m(1-t)B\big)\big)\,\kappa_\alpha(t)\,dt \le H_\alpha(h,s)\,\lambda_k(\varphi(A)) + m\,\widetilde{H}_\alpha(h,s)\,\lambda_k(\varphi(B)).$$

Such eigenvalue-level certificates are useful when the objective depends on the spectrum rather than only on the trace.

Kubo–Ando theory provides an axiomatic framework for matrix means on $\mathbb{H}_d^{++}$. In the commuting regime, these means reduce to their scalar counterparts applied eigenvalue-wise. However, a general Kubo–Ando mean is not necessarily the modified affine combination $\theta a + m(1-\theta)b$. Therefore, an explicit scalar compatibility condition is required before the modified (h,m)–convexity inequality can be applied.

Corollary 6.6 (Trace certificate for commuting Kubo–Ando means)**.** *Let $A, B \in \mathbb{H}_d^{++}$ commute, and let σ_θ be a Kubo–Ando mean indexed by $\theta \in [0,1]$. Let $\varphi : (0,\infty) \to \mathbb{R}$ be a scalar function. Suppose that the scalar mean associated with σ_θ is compatible with the modified (h,m)–convexity structure in the sense that, for all $a, b > 0$,*

$$\varphi(a\sigma_\theta b) \le h(\theta)^s\,\varphi(a) + m\big(1-h(\theta)\big)^s\,\varphi(b). \tag{35}$$

Then

$$\mathrm{tr}\big(\varphi(A\sigma_\theta B)\big) \le h(\theta)^s\ \mathrm{tr}(\varphi(A)) + m\big(1-h(\theta)\big)^s\ \mathrm{tr}(\varphi(B)). \tag{36}$$

Proof. Since A and B commute, there exists a unitary matrix U such that

$$A = U\,\mathrm{diag}(a_1,\dots,a_d)U^*, \qquad B = U\,\mathrm{diag}(b_1,\dots,b_d)U^*,$$

with $a_i, b_i > 0$ for all i. By the commuting reduction property of Kubo–Ando means,

$$A\sigma_\theta B = U\,\mathrm{diag}\big(a_i\sigma_\theta b_i\big)_{i=1}^{d} U^*,$$

where $a_i\sigma_\theta b_i$ denotes the corresponding scalar mean. Applying the scalar compatibility condition (35) to each pair (a_i, b_i) gives

$$\varphi(a_i\sigma_\theta b_i) \le h(\theta)^s\,\varphi(a_i) + m\big(1-h(\theta)\big)^s\,\varphi(b_i), \qquad i = 1,\dots,d.$$

Summing over i and using the trace representation under simultaneous diagonalization yields (36). □

For noncommuting matrices, the scalar-to-operator lift is not automatic and must therefore be imposed as a hypothesis.

Theorem 6.7 (HH–F trace bound under operator modified (h, m)–convexity)**.** *Assume Assumption 2.6. Let φ be operator modified (h, m)–convex of the second type with parameter s in the sense of Definition 6.1. Then, for all $A, B \in \mathbb{H}_d^{++}$, not necessarily commuting, and every $\alpha > 0$,*

$$\int_0^1 \operatorname{tr}\big(\varphi\big(tA + m(1-t)B\big)\big)\, \kappa_\alpha(t)\, dt \le H_\alpha(h,s)\ \operatorname{tr}(\varphi(A)) + m\, \widetilde{H}_\alpha(h,s)\ \operatorname{tr}(\varphi(B)). \tag{37}$$

Proof. For each $t \in [0,1]$, Definition 6.1 gives

$$\varphi\big(tA + m(1-t)B\big) \preceq h(t)^s\, \varphi(A) + m\big(1-h(t)\big)^s\, \varphi(B).$$

As in the proof of Theorem 6.4, multiply by the nonnegative kernel $\kappa_\alpha(t)$, take traces, and integrate over $t \in [0,1]$. The resulting coefficients are precisely the kernel averages $H_\alpha(h,s)$ and $\widetilde{H}_\alpha(h,s)$. □

Remark 6.8 (Scope of the noncommuting result). Theorem 6.7 is deliberately stated as an implication rather than as a general lift theorem. Its content is that, once the operator compatibility condition (32) is available, the HH–F trace mechanism extends in the same manner as in the scalar case. In applications, the most practically verifiable situations remain those in which the relevant matrices commute or are jointly diagonalizable, in which case the fully rigorous commuting theory developed above applies directly.

7. NUMERICAL ILLUSTRATIONS AND CERTIFICATE VALIDATION

A recurring expectation in inequality-driven methodology is that the resulting constants should be explicitly computable, the bounds should be verifiable from finite data, and the numerical section should demonstrate not only validity but also interpretability. In the present framework, the only nontrivial coefficients are the one-dimensional kernel averages

$$H_\alpha(h,s) = \int_0^1 h(t)^s\, \kappa_\alpha(t)\, dt, \qquad \widetilde{H}_\alpha(h,s) = \int_0^1 \big(1-h(t)\big)^s\, \kappa_\alpha(t)\, dt,$$

where κ_α is the Fejér-symmetric kernel from Definition 2.8. These quantities are dimension-free and can therefore be precomputed once for fixed (α, h, s) and then reused in the multivariate box certificates of Section 4 and the commuting trace bounds of Section 6.

To make the numerical validation independent of the theorem statements themselves, we employ a uniform verification protocol. Whenever closed-form integration is available, we compute the exact average and report the corresponding certificate gap, that is, the difference between the certificate and the true average. When closed forms are unavailable, we approximate kernel-weighted averages by high-order Gaussian quadrature. For one-dimensional integrals in t, Gauss–Jacobi rules are used to accommodate endpoint behavior of the form $t^{\alpha-1}$ and $(1-t)^{\alpha-1}$; for tensorized kernels, tensor-product quadrature is used in the variables $(t_1, \ldots, t_n)$. As an additional numerical check, we verify each inequality by Monte Carlo sampling of 10^5 uniformly distributed points on the underlying domain, or along the scalar or matrix path in the commuting examples, and compare the empirical mean with the corresponding certificate. In all reported experiments, the certificate remains above the empirical mean with a stable positive gap. All computations are performed in double precision, and the reported digits are stable under refinement of the quadrature order and the random seeds.

To complement these experiment-specific checks, it is also useful to examine the numerical behavior of the kernel coefficients themselves. Since the constants $H_\alpha(h,s)$ and $\widetilde{H}_\alpha(h,s)$ are one-dimensional and dimension-free, their evaluation is computationally negligible, yet they govern the sharpness of the resulting certificates. We begin with the canonical case $h(t) = t$, for which closed forms are available and can be tabulated explicitly.

We begin with a practically important specialization that covers the classical HH–F regime as well as many standard weighted variants.

Proposition 7.1 (Computable constants for $h(t) = t$)**.** *Let $h(t) = t$ and assume $s > -1$ and $\alpha + s > 0$. Then, for every $\alpha > 0$,*

$$\begin{aligned} H_\alpha(\mathrm{id}, s) &= \frac{\alpha}{2}\left(\int_0^1 t^{\alpha+s-1}\, dt + \int_0^1 t^s (1-t)^{\alpha-1}\, dt\right) \\ &= \frac{\alpha}{2}\left(\frac{1}{\alpha+s} + \mathrm{B}(s+1, \alpha)\right), \end{aligned} \tag{38}$$

$$\begin{aligned} \widetilde{H}_\alpha(\mathrm{id}, s) &= \frac{\alpha}{2}\left(\int_0^1 (1-t)^{\alpha+s-1}\, dt + \int_0^1 (1-t)^s t^{\alpha-1}\, dt\right) \\ &= \frac{\alpha}{2}\left(\frac{1}{\alpha+s} + \mathrm{B}(\alpha, s+1)\right), \end{aligned} \tag{39}$$

where B *denotes the Beta function. In particular, when* $\alpha = 1$*,*

$$\kappa_1(t) \equiv 1, \qquad H_1(\mathrm{id}, s) = \widetilde{H}_1(\mathrm{id}, s) = \int_0^1 t^s \, dt = \frac{1}{s+1}. \tag{40}$$

Proof. The formulas follow directly by substituting

$$\kappa_\alpha(t) = \frac{\alpha}{2}\left(t^{\alpha-1} + (1-t)^{\alpha-1}\right)$$

into the definitions of H_α and $\widetilde{H}_\alpha$, and then identifying the mixed terms with Beta-function integrals. □

Remark 7.2 (Precomputation beyond $h(t) = t$). For general h and s, the quantities $H_\alpha(h, s)$ and $\widetilde{H}_\alpha(h, s)$ remain one-dimensional integrals over a fixed interval, and their numerical cost is negligible compared with the 2^n vertex evaluations appearing in Theorem 4.1. In practice, Gauss–Jacobi quadrature is especially effective because it is naturally adapted to the endpoint behavior of κ_α.

To make Proposition 7.1 more concrete, Table 1 provides representative instances of the kernel coefficients for canonical choices of the parameters. Even for the basic special case $h(t) = t$, the table demonstrates the dependence of the constants on the parameters α and s. It also shows that the constants are easy to precompute and reuse for different problem instances.

Table 1. *Representative closed-form kernel coefficients from Proposition 7.1 for the canonical choice* $h(t) = t$

α	s	$H_\alpha(\mathrm{id}, s)$	$\widetilde{H}_\alpha(\mathrm{id}, s)$
1	1	0.5000	0.5000
1	2	0.3333	0.3333
2	1	0.5000	0.5000
3	1	0.5000	0.5000
2	2	0.3333	0.3333

We first validate the vertex certificate from Section 4 on a smooth convex surface. To avoid any ambiguity related to generalized convexity assumptions, we work in the classical specialization $m = s = 1$, $h(t) = t$, $\alpha_i = 1$, and $w_i(t) = t$.

Example 7.3 (Quadratic loss on a box)**.** Let

$$f(x, y) = x^2 + y^2 + 1 \quad \text{on} \quad \mathcal{B}((1, 1)) = [0, 1]^2.$$

Choose $m = 1$, $h(t) = t$, $s = 1$, $w_1 = w_2 = \mathrm{id}$, and $\alpha_1 = \alpha_2 = 1$. Then $\kappa_1(t) \equiv 1$, and Proposition 7.1 gives

$$H_1 = \widetilde{H}_1 = \frac{1}{2},$$

so that $C_{\boldsymbol{\varepsilon}} = 2^{-2}$ for all $\boldsymbol{\varepsilon} \in \{0, 1\}^2$. Theorem 4.1 yields the certificate

$$\frac{1}{\mathrm{vol}([0, 1]^2)} \int_{[0,1]^2} f(x, y) \, dx \, dy \le \frac{1}{4} \sum_{\boldsymbol{\varepsilon} \in \{0,1\}^2} f(v_{\boldsymbol{\varepsilon}}). \tag{41}$$

A direct computation gives

$$\frac{1}{\mathrm{vol}([0, 1]^2)} \int_{[0,1]^2} f(x, y) \, dx \, dy = 1 + \frac{1}{3} + \frac{1}{3} = \frac{5}{3} \approx 1.6667,$$

whereas the vertex certificate equals

$$\frac{1}{4}\big(f(0, 0) + f(1, 0) + f(0, 1) + f(1, 1)\big) = \frac{1}{4}(1 + 2 + 2 + 3) = 2.$$

Thus, the certificate gap is

$$2 - \frac{5}{3} = \frac{1}{3} \approx 0.3333.$$

Figure 1 visualizes the geometry of the loss surface and the role of the vertices in the resulting certificate.

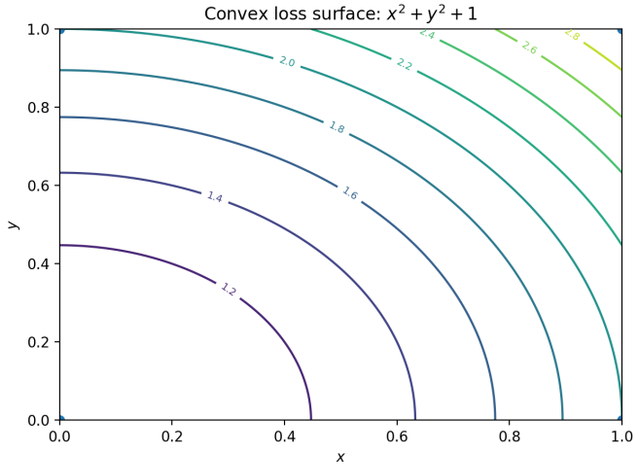

Figure 1. *Contour plot of the convex loss $f(x, y) = x^2 + y^2 + 1$ on $[0, 1]^2$ with vertices highlighted. Theorem 4.1 bounds the average using only vertex values.*

To complement the exact calculation in Example 7.3, Table 2 reports the exact average, the vertex-based certificate, the resulting gap, and the corresponding Monte Carlo estimate. The empirical mean serves only as an external numerical check and is not used in the proof of the inequality. As the table shows, the Monte Carlo estimate closely matches the exact average, while the certificate remains strictly above the mean, confirming the validity of the bound and illustrating the conservative yet numerically stable nature of the estimate.

Table 2. *Numerical verification of the bivariate certificate in Example 7.3*

Quantity	**Value**
Exact average	1.6667
Vertex certificate	2.0000
Certificate gap	0.3333
Monte Carlo mean (10^5 samples)	1.6671

This benchmark confirms the expected behavior of the classical box certificate in a setting where all quantities are analytically available. It also provides a useful baseline against which the applied examples below may be interpreted.

Matrix-valued energies and barrier-type functionals arise naturally in control, optimization, and signal processing. In the commuting regime, the trace inequality from Section 6 yields explicit certificates along affine matrix paths.

Example 7.4 (A commuting trace HH–F certificate)**.** Let

$$A = \operatorname{diag}(1, 4), \qquad B = \operatorname{diag}(2, 3),$$

so that A and B commute. Take $\varphi(t) = t^2$, $m = s = 1$, $h(t) = t$, and $\alpha = 1$, so that $\kappa_1(t) \equiv 1$ and $H_1 = \widetilde{H}_1 = \frac{1}{2}$. Theorem 6.4 yields

$$\int_0^1 \operatorname{tr}\big((tA + (1-t)B)^2\big)\, dt \le \frac{1}{2}\operatorname{tr}(A^2) + \frac{1}{2}\operatorname{tr}(B^2). \tag{42}$$

Now

$$\operatorname{tr}\big((tA + (1-t)B)^2\big) = (2-t)^2 + (3+t)^2 = 13 + 2t + 2t^2,$$

so that

$$\int_0^1 \operatorname{tr}\big((tA + (1-t)B)^2\big)\, dt = \int_0^1 (13 + 2t + 2t^2)\, dt = 13 + 1 + \frac{2}{3} = \frac{44}{3} \approx 14.667.$$

On the other hand,

$$\frac{1}{2}\operatorname{tr}(A^2) + \frac{1}{2}\operatorname{tr}(B^2) = \frac{1}{2}(17) + \frac{1}{2}(13) = 15.$$

Hence, the trace certificate gap is

$$15 - \frac{44}{3} = \frac{1}{3} \approx 0.3333.$$

Figure 2 displays the path integrand together with the certificate level.

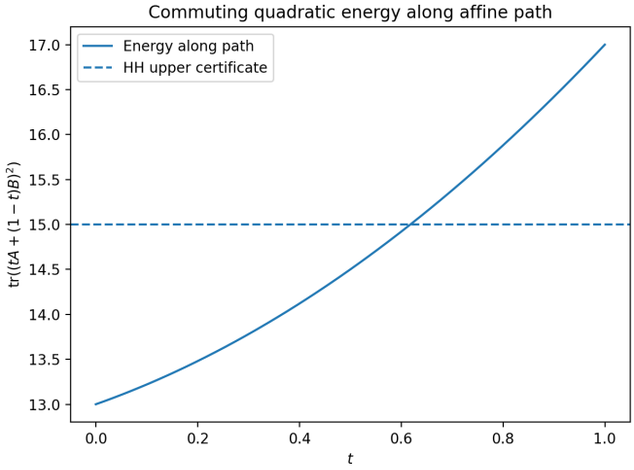

Figure 2. *Commuting matrix example from Example 7.4: the integrand* $t \mapsto \operatorname{tr}((tA + (1-t)B)^2)$ *and the HH upper certificate* $\frac{1}{2}\operatorname{tr}(A^2) + \frac{1}{2}\operatorname{tr}(B^2)$.

Table 3 summarizes the numerical verification of the commuting trace certificate from Example 7.4. The Monte Carlo estimate closely matches the exact integral, while the trace-based certificate remains strictly above the empirical mean. As in the scalar case, this confirms the validity and numerical stability of the operator inequality in the commuting matrix setting.

Table 3. *Numerical verification of the commuting trace certificate in Example 7.4*

Quantity	**Value**
Exact integral	14.6667
Trace certificate	15.0000
Certificate gap	0.3333
Monte Carlo mean (10^5 samples)	14.6710

This example shows that the commuting matrix theory yields certificates that are as explicit and interpretable as their scalar counterparts. In particular, only endpoint traces are needed, while the averaged path quantity is controlled rigorously.

The previous examples verify the mathematical certificates in simple benchmark settings. We now indicate several applied contexts in which the same bounds provide interpretable conservative surrogates for averaged objectives. These examples are intended as illustrative uses of the certificates rather than as full engineering validation studies.

To make the discussion of applications more informative from a numerical point of view, we again state the exact average values, certified bounds, and certificate gaps. This allows comparison of the conservatism of the certificates for different classes of applications.

Application I: Economic dispatch cost envelopes. Quadratic generation cost models are standard in economic dispatch and related optimization problems. When generation setpoints lie in a box, Theorem 4.1 gives a conservative upper certificate for the average cost using only vertex values.

Example 7.5 (Two-generator convex cost on a box)**.** Let $(p_1, p_2) \in [0,1]^2$ denote per-unit generator outputs, and consider

$$C(p_1, p_2) = a_1 p_1^2 + b_1 p_1 + a_2 p_2^2 + b_2 p_2$$

with

$$(a_1, b_1, a_2, b_2) = (0.9, 0.2, 1.2, 0.1).$$

Under the classical specialization $m = s = 1$, $h(t) = t$, $\alpha_i = 1$, and $w_i = \mathrm{id}$, Theorem 4.1 gives

$$\frac{1}{\operatorname{vol}([0,1]^2)} \int_{[0,1]^2} C(p_1, p_2)\, dp_1\, dp_2 \le \frac{1}{4} \sum_{\varepsilon \in \{0,1\}^2} C(v_\varepsilon).$$

The exact average is

$$\frac{1}{\operatorname{vol}([0,1]^2)} \int_{[0,1]^2} C = \frac{a_1}{3} + \frac{b_1}{2} + \frac{a_2}{3} + \frac{b_2}{2} = 0.85,$$

whereas the vertex certificate equals

$$\frac{1}{4}(0 + 1.1 + 1.3 + 2.4) = 1.2.$$

Thus, the certificate gap is

$$1.2 - 0.85 = 0.35.$$

Figure 3 shows the cost surface and the location of the vertices. This certificate may be used as a screening certificate for box-constrained uncertainty sets.

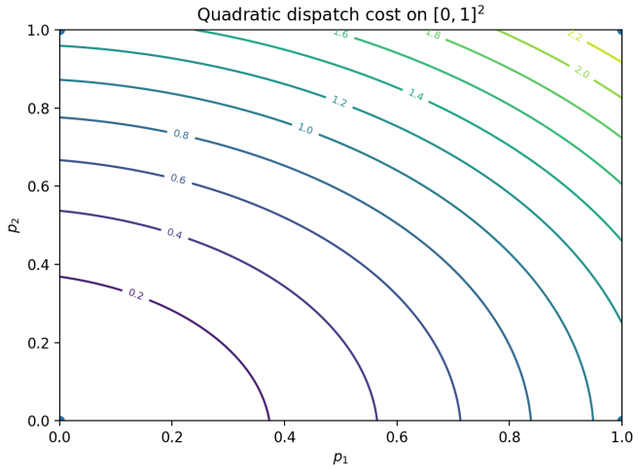

Figure 3. *Economic-dispatch surrogate cost from Example 7.5 on* $[0,1]^2$ *with vertices highlighted. Theorem 4.1 provides a vertex-only upper certificate for the average cost.*

The numerical verification of the certificate derived in Example 7.5 is provided in Table 4. The Monte Carlo estimate closely approximates the exact average cost, while the vertex-based certificate remains safely above the empirical mean. This certificate gap demonstrates the conservative yet interpretable nature of the derived estimate.

Table 4. *Numerical verification of the economic dispatch certificate in Example 7.5*

Quantity	**Value**
Exact average cost	0.8500
Vertex certificate	1.2000
Certificate gap	0.3500
Monte Carlo mean (10^5 samples)	0.8520

Application II: Stored-energy envelopes in RLC models. Energy functions are important tools in circuit modeling and passivity-based analysis. When currents and voltages are restricted to a design box, HH-type bounds provide conservative certificates for the average energy [11, 3, 22].

Example 7.6 (RLC stored energy on a magnitude box)**.** Consider the energy

$$E(i,v) = \frac{1}{2}Li^2 + \frac{1}{2}Cv^2, \qquad (i,v) \in [0,1]^2,$$

with $(L,C) = (1.5, 0.8)$. Under the classical specialization, Theorem 4.1 yields

$$\frac{1}{\mathrm{vol}([0,1]^2)} \int_{[0,1]^2} E(i,v)\, di\, dv \le \frac{1}{4}\big(E(0,0) + E(1,0) + E(0,1) + E(1,1)\big).$$

The exact average is

$$\frac{1}{\mathrm{vol}([0,1]^2)} \int_{[0,1]^2} E = \frac{L+C}{6} \approx 0.3833,$$

while the vertex certificate equals

$$\frac{1}{4}\left(0 + \frac{1}{2}L + \frac{1}{2}C + \frac{1}{2}(L+C)\right) = 0.575.$$

Hence, the certificate gap is approximately

$$0.575 - 0.3833 \approx 0.1917.$$

Figure 4 shows the corresponding energy contours. Such bounds may be interpreted as conservative energy envelopes on bounded operating regions.

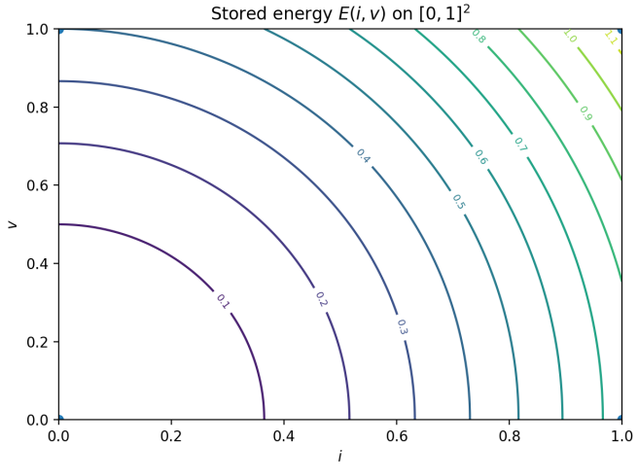

Figure 4. *Stored energy* $E(i, v) = \frac{1}{2}Li^2 + \frac{1}{2}Cv^2$ *on* $[0, 1]^2$ *in Example 7.6, with vertices highlighted.*

Table 5 shows the numerical verification of the certificate developed in Example 7.6. The Monte Carlo approximation is close to the exact average energy, while the vertex-based certificate remains above the empirical mean. Among the examples treated in this section, the certificate gap is relatively small because of the moderate curvature of the energy surface on the box.

Table 5. *Numerical verification of the RLC energy certificate in Example 7.6*

Quantity	**Value**
Exact average energy	0.3833
Vertex certificate	0.5750
Certificate gap	0.1917
Monte Carlo mean (10^5 samples)	0.3841

Application III: Log-determinant certificates in covariance design. Log-determinant quantities arise in covariance design, barrier methods, and information-theoretic models. In the commuting regime, Section 6 provides a rigorous certificate for averages along affine covariance paths.

Example 7.7 (Commuting log-det barrier along an affine path)**.** Let

$$A = \operatorname{diag}(1.2, 2.5, 4.0), \qquad B = \operatorname{diag}(2.0, 1.8, 3.2),$$

and consider the convex functional

$$\psi(X) = -\log\det(X).$$

Since A and B commute, the classical specialization $m = s = 1$, $h(t) = t$, and $\alpha = 1$ yields

$$\int_0^1 \big(-\log\det(tA + (1-t)B)\big)\, dt \le \frac{1}{2}\big(-\log\det A\big) + \frac{1}{2}\big(-\log\det B\big).$$

Numerically,

$$\int_0^1 \big(-\log\det(tA + (1-t)B)\big)\, dt \approx -2.4993,$$

and

$$\frac{1}{2}\big(-\log\det A - \log\det B\big) \approx -2.4645.$$

Hence, the certificate gap is approximately

$$-2.4645 - (-2.4993) = 0.0348.$$

Figure 5 visualizes the barrier along the commuting affine path. In applications, such a bound provides a conservative certificate for average log-det penalties under interpolated covariance policies.

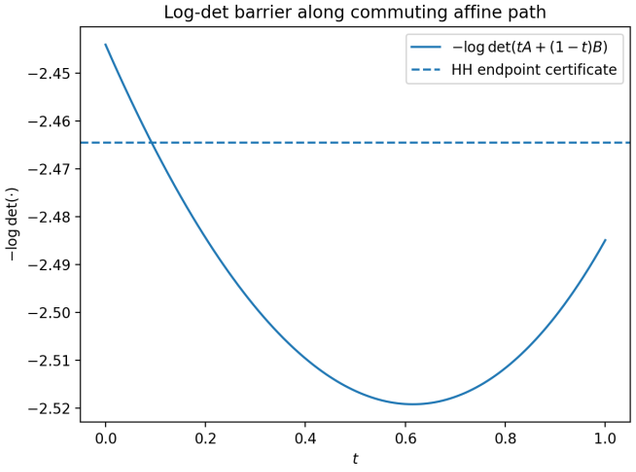

Figure 5. *Log-determinant barrier along a commuting affine path in Example 7.7, together with the endpoint-based HH upper certificate.*

Table 6. *Numerical verification of the log-determinant certificate in Example 7.7*

Quantity	Value
Exact integral	-2.4993
HH certificate	-2.4645
Certificate gap	0.0348
Monte Carlo mean (10^5 samples)	-2.4989

A summary of the numerical verification for the certificate computed in Example 7.7 is provided in Table 6. The Monte Carlo estimate is close to the exact integral computation, whereas the HH certificate remains above the empirical mean. In relative error, this is the strongest certificate computed for this example, suggesting that endpoint-based HH bounds may be particularly effective for smoothly varying commuting matrix barriers.

To facilitate comparison, Table 7 summarizes the most important numerical results from the benchmark and application problems. This provides better insight into the variability of certificate conservativeness for scalar, multivariate, and matrix problems.

Table 7. *Summary of exact averages, certificates, and certificate gaps across the numerical examples*

Example	Exact / true average	Certificate	Gap
Quadratic loss (Example 7.3)	1.6667	2.0000	0.3333
Commuting trace (Example 7.4)	14.6667	15.0000	0.3333
Economic dispatch (Example 7.5)	0.8500	1.2000	0.3500
RLC energy (Example 7.6)	0.3833	0.5750	0.1917
Log-det barrier (Example 7.7)	-2.4993	-2.4645	0.0348

The explicit computability of the kernel coefficients and the vertex-based nature of the resulting bounds make the framework appealing for certificate-driven workflows, including quadrature validation, uncertainty-aware design-space exploration, and surrogate evaluation of integral objectives in optimization.

The numerical experiments collectively validate the theoretical guarantees provided in Sections 4 and 6. In all instances examined here, the certificate is a valid upper bound on the respective average value, and the independently computed Monte Carlo estimates remain below the respective certified threshold. From a computational point of view, the numerical experiments also verify that the method is computationally simple to implement, since the only nontrivial coefficients are one-dimensional averages over a kernel function, whereas the final certificates depend only on endpoint or vertex data.

8. ILLUSTRATIVE AND COMPUTATIONAL EXAMPLES: THE ROLE OF THE GENERALIZED PARAMETERS

The preceding sections develop a kernel-weighted Hermite–Hadamard–Fejér framework under modified (h, m)–convexity and derive explicit certificates in one-dimensional, multivariate, and commuting matrix settings. The purpose of the present section is to make the role of the generalized parameters concrete. In particular, the examples below show that the parameters h, m, s, and the weight maps w_i are not merely formal generalizations: they determine the admissible function class, the geometry of the averaging rule, and the numerical conservatism of the resulting certificates.

From a computational point of view, these parameters may be interpreted as modeling and certification controls. The exponent parameter s adjusts curvature sensitivity, the scaling parameter m controls asymmetric endpoint influence, and the maps w_i induce nonuniform sampling rules adapted to the expected behavior of the integrand. Consequently, the theory yields not only abstract inequalities, but also tunable and numerically checkable bounds that can be tailored to structured averaging and certificate-based validation tasks.

Parameter s as a curvature modulator. We begin with a standard family that shows how the exponent s enlarges the admissible class beyond classical convexity.

Example 8.1 (Power-law model under nonclassical curvature weighting)**.** Let $h(t) = t$, $m = 1$, and consider

$$f(x) = x^p, \qquad x \geq 0, \qquad 0 < p \leq 1.$$

For $\gamma \in [0, 1]$ and $x, y \geq 0$, the modified (h, m)–convexity condition reduces to

$$(\gamma x + (1-\gamma)y)^p \leq \gamma^s x^p + (1-\gamma)^s y^p.$$

Choosing $s = p$ gives

$$(\gamma x + (1-\gamma)y)^p \leq \gamma^p x^p + (1-\gamma)^p y^p,$$

which follows from the subadditivity of the map $u \mapsto u^p$ on $[0, \infty)$. Thus, for $0 < p < 1$, the framework captures concave power laws that lie outside the classical convex class.

This observation is useful in applied settings where response laws exhibit diminishing returns or saturation. In such cases, the parameter s acts as a curvature modulator, allowing the certification framework to remain applicable even when standard convexity is unavailable.

Parameter m as an asymmetric scaling factor. The parameter $m \in (0, 1]$ modifies the contribution of the second endpoint and is particularly natural on domains anchored at the origin.

Example 8.2 (Asymmetric mixing induced by $m < 1$)**.** Let $h(t) = t$, $s = 1$, $m = \frac{1}{2}$, and consider

$$f(x) = x^2, \qquad x \in [0, 1].$$

Then the modified convexity inequality becomes

$$\left(\gamma x + \frac{1}{2}(1-\gamma)y\right)^2 \leq \gamma x^2 + \frac{1}{2}(1-\gamma)y^2, \qquad \gamma \in [0, 1].$$

Indeed, setting $\beta = \frac{1}{2}(1-\gamma)$, we have $\gamma + \beta \leq 1$, and by the Cauchy–Schwarz inequality,

$$(\gamma x + \beta y)^2 \leq (\gamma + \beta)(\gamma x^2 + \beta y^2) \leq \gamma x^2 + \beta y^2.$$

Hence, f satisfies the modified (h, m)–convexity condition with a reduced influence of the second endpoint.

This example shows that m is not merely a notational variant of the classical parameterization. It provides a controlled asymmetry in the averaging process, which is useful in applications where one endpoint represents a damped, discounted, or otherwise attenuated state.

Nonuniform weight maps and adaptive averaging. The weight maps w_i alter the pullback geometry of the integral operator and therefore change the effective sampling profile of the certificate.

Example 8.3 (A nonuniform averaging rule generated by $w(t) = t^2$)**.** Consider the interval $[0, 1]$ and the increasing map

$$w(t) = t^2, \qquad 0 \leq t \leq 1.$$

Its pullback is

$$\xi(u) = \sqrt{u}, \qquad 0 \leq u \leq 1.$$

For $\alpha = 1$, the kernel satisfies $\kappa_1(t) \equiv 1$, so the corresponding operator becomes

$$\mathcal{I}_{1,w}[f; 0, 1] = \int_0^1 f(\sqrt{u})\, du.$$

Taking $f(x) = x^2$, we obtain

$$\mathcal{I}_{1,w}[f;0,1] = \int_0^1 (\sqrt{u})^2\,du = \int_0^1 u\,du = \frac{1}{2},$$

whereas the classical Lebesgue average is

$$\int_0^1 x^2\,dx = \frac{1}{3}.$$

Thus, the nonuniform map w increases the effective emphasis on larger argument values. In the classical specialization $h(t) = t$, $m = 1$, and $s = 1$, Theorem 3.1 yields the certificate

$$\mathcal{I}_{1,w}[f;0,1] \le \frac{1}{2}f(1) + \frac{1}{2}f(0) = \frac{1}{2},$$

which is attained in this case.

From a computational perspective, this example shows that the choice of w directly changes the averaging rule and the resulting conservatism. Hence, the maps w_i can be viewed as adaptive sampling devices within the certificate construction.

A numerically verified nonclassical one-dimensional certificate. We now present a one-dimensional example in which the generalized parameters produce a valid nonclassical certificate for a function that is not classically convex.

Example 8.4 (Square-root response under $s = \frac{1}{2}$)**.** Let

$$f(x) = \sqrt{x}, \qquad x \in [0,1],$$

and choose

$$h(t) = t, \qquad m = 1, \qquad s = \frac{1}{2}.$$

Then, for all $\gamma \in [0,1]$ and $x, y \ge 0$,

$$(\gamma x + (1-\gamma)y)^{1/2} \le \gamma^{1/2}x^{1/2} + (1-\gamma)^{1/2}y^{1/2},$$

so f satisfies the modified convexity condition in the form relevant to Definition 2.1.

For $\alpha = 1$ and the identity map $w(t) = t$, Theorem 3.1 gives

$$\int_0^1 \sqrt{t}\,dt \le H_1(\mathrm{id}, \tfrac{1}{2})f(1) + \widetilde{H}_1(\mathrm{id}, \tfrac{1}{2})f(0).$$

Since

$$H_1(\mathrm{id}, \tfrac{1}{2}) = \int_0^1 t^{1/2}\,dt = \frac{2}{3}, \qquad \widetilde{H}_1(\mathrm{id}, \tfrac{1}{2}) = \int_0^1 (1-t)^{1/2}\,dt = \frac{2}{3},$$

and $f(1) = 1$, $f(0) = 0$, the certificate becomes

$$\int_0^1 \sqrt{t}\,dt \le \frac{2}{3}.$$

The left-hand side is exactly

$$\int_0^1 \sqrt{t}\,dt = \frac{2}{3},$$

so the bound is sharp.

This example is computationally important because the certificate constants are explicit and the bound is immediately verifiable. It also shows that the framework can produce exact certificates for nonclassical response laws.

A multivariate vertex certificate. The next example illustrates how the one-dimensional constants propagate into the tensorized box certificate.

Example 8.5 (Bivariate certificate with nonclassical parameter choice)**.** Consider

$$f(x,y) = \sqrt{x} + \sqrt{y}, \qquad (x,y) \in [0,1]^2,$$

with the same parameter choice as in Example 8.4:

$$h(t) = t, \qquad m = 1, \qquad s = \frac{1}{2}, \qquad \alpha_1 = \alpha_2 = 1, \qquad w_1 = w_2 = \mathrm{id}\,.$$

The function is not classically convex on $[0,1]^2$, but it is coordinate-wise compatible with the modified framework induced by $s = \frac{1}{2}$.

The exact average is

$$\mathcal{I}_{\boldsymbol{\alpha},\mathbf{w}}[f;[0,1]^2] = \int_0^1 \int_0^1 (\sqrt{x} + \sqrt{y})\, dx\, dy = \frac{4}{3}.$$

Moreover,

$$c_i(1) = H_1(\mathrm{id}, \tfrac{1}{2}) = \frac{2}{3}, \qquad c_i(0) = \widetilde{H}_1(\mathrm{id}, \tfrac{1}{2}) = \frac{2}{3},$$

so every vertex coefficient is

$$C_{\boldsymbol{\varepsilon}} = \prod_{i=1}^{2} c_i(\varepsilon_i) = \frac{4}{9}.$$

Since the vertex values are

$$f(0,0) = 0, \qquad f(1,0) = 1, \qquad f(0,1) = 1, \qquad f(1,1) = 2,$$

Theorem 4.1 yields the certificate

$$\sum_{\boldsymbol{\varepsilon}\in\{0,1\}^2} C_{\boldsymbol{\varepsilon}} f(v_{\boldsymbol{\varepsilon}}) = \frac{4}{9}(0+1+1+2) = \frac{16}{9}.$$

Hence

$$\frac{4}{3} \le \frac{16}{9}.$$

This example illustrates the computational structure of the multivariate theory: once the one-dimensional constants are known, the box certificate is assembled from endpoint data only. This feature is valuable when full multidimensional integration is expensive but vertex evaluations are readily available.

A commuting matrix trace certificate. Finally, we illustrate the commuting matrix regime, which is the rigorous operator setting developed in Section 6.

Example 8.6 (Trace certificate for a commuting positive-definite pair)**.** Let

$$A = \mathrm{diag}(1,4), \qquad B = \mathrm{diag}(2,3),$$

and let $\varphi(t) = \sqrt{t}$. Using again

$$h(t) = t, \qquad m = 1, \qquad s = \frac{1}{2},$$

the scalar inequality from Example 8.4 transfers to the commuting matrix setting considered in Section 6.

For $\alpha = 1$, Theorem 6.4 gives

$$\int_0^1 \mathrm{tr}\Big((tA + (1-t)B)^{1/2}\Big)\, dt \le H_1(\mathrm{id}, \tfrac{1}{2})\,\mathrm{tr}(A^{1/2}) + \widetilde{H}_1(\mathrm{id}, \tfrac{1}{2})\,\mathrm{tr}(B^{1/2}).$$

Since

$$H_1(\mathrm{id}, \tfrac{1}{2}) = \widetilde{H}_1(\mathrm{id}, \tfrac{1}{2}) = \frac{2}{3},$$

and

$$A^{1/2} = \mathrm{diag}(1,2), \qquad \mathrm{tr}(A^{1/2}) = 3,$$

$$B^{1/2} = \mathrm{diag}(\sqrt{2},\sqrt{3}), \qquad \mathrm{tr}(B^{1/2}) = \sqrt{2} + \sqrt{3} \approx 3.1463,$$

the right-hand side is

$$\frac{2}{3}\big(3 + \sqrt{2} + \sqrt{3}\big) \approx 4.0975.$$

For the left-hand side, because A and B commute,

$$tA + (1-t)B = \mathrm{diag}(2-t, 3+t).$$

Hence

$$\int_0^1 \operatorname{tr}\Big((tA+(1-t)B)^{1/2}\Big)\,dt = \int_0^1 \big(\sqrt{2-t}+\sqrt{3+t}\big)\,dt = \frac{2}{3}\big(7+2\sqrt{2}-3\sqrt{3}\big) \approx 3.0882.$$

Therefore,

$$3.0882 \le 4.0975,$$

which confirms the certificate.

This example is computationally relevant because the trace bound is obtained from explicit scalar coefficients and endpoint matrix data. It illustrates the practical value of the commuting theory for certified bounds on structured matrix averages.

Examples 8.1–8.6 clarify the distinct roles of the generalized parameters. The exponent s broadens the admissible curvature class, the factor m introduces asymmetric mixing, and the maps w_i generate nonuniform averaging rules adapted to the intended sampling profile. In addition, the one-dimensional constants H_α and $\widetilde{H}_\alpha$ are explicit and reusable, so the resulting certificates can be assembled with low online cost once the parameter choice has been fixed.

From the perspective of computational and applied mathematics, the main practical message is that the framework converts generalized convexity assumptions into numerically checkable certificate formulas. In one dimension, this yields direct average bounds; in boxes, it produces endpoint-driven surrogate certificates; and in the commuting matrix setting, it furnishes tractable trace bounds for structured positive-definite mixtures. Thus, the generalized parameters are not ornamental: they are operational tools that tailor the inequality to the geometry, curvature profile, and computational objectives of the problem under study.

9. IMPLICATIONS FOR OPTIMIZATION AND COMPUTATIONAL WORKFLOWS

The results developed in this paper are most naturally interpreted as *certificate tools* for computational and applied mathematics rather than as stand-alone optimization algorithms. In this perspective, the kernel-weighted HH–F bounds support three complementary computational roles: they provide *upper certificates for regional averages*, *conservative surrogate bounds for screening and pruning*, and *reusable quadrature-aware constants* that can be precomputed independently of the ambient dimension. The illustrative examples of Section 8 further show that the generalized parameters are not merely formal extensions: they influence the admissible curvature class, the averaging geometry, and the conservatism of the resulting certificates.

For objectives of the form

$$\int_{\mathcal{B}(\mathbf{b})} f(\mathbf{x})\,d\mu(\mathbf{x}),$$

where μ is a product kernel measure defined by $(\boldsymbol{\alpha}, \mathbf{w})$, Theorem 4.1 yields a vertex-only upper certificate. This is computationally attractive in box-constrained settings because the bound depends only on endpoint data and one-dimensional kernel coefficients. Such certificates may therefore serve as conservative surrogates in branch-and-bound procedures, region-pruning strategies, and mixed-integer outer-approximation schemes, where sub-boxes preserve their structure under affine coordinate transformations. In that setting, the certificate may be used to discard regions whose certified average value is already too large for the surrounding optimization task [2]. The economic-dispatch illustration in Section 7 should be understood in precisely this sense: as a certificate-style surrogate for bounded scenarios, not as a complete dispatch algorithm.

The choice of the coordinate maps w_i accommodates graded meshes and nonuniform coordinate transformations, making $\mathcal{I}_{\boldsymbol{\alpha},\mathbf{w}}$ a flexible substitute for uniform averaging rules. As illustrated in Section 8, these maps can also be interpreted as adaptive sampling profiles that shift the effective emphasis of the integral operator toward different parts of the domain. In parallel, the generalized parameters h, m, and s control the admissible convexity structure: the exponent s modulates curvature sensitivity, while the factor m introduces asymmetric mixing. This additional flexibility is important in computational practice because it allows the certificate to be matched more closely to the structure of the modeled response.

A further computational advantage is the implicit offline-online decomposition built into the theory. The constants $H_{\alpha_i}(h,s)$ and $\widetilde{H}_{\alpha_i}(h,s)$ are one-dimensional quantities that do not depend on the ambient dimension n; see Proposition 7.1. Once the parameter choice has been fixed, these coefficients can be precomputed offline and then reused across multiple boxes, uncertainty sets, or related scenarios that share the same kernel structure. In this way, the multidimensional certificate construction is reduced to a combination of reusable scalar constants and boundary evaluations, which is often substantially cheaper than repeated full-dimensional integration.

In the commuting matrix regime, Theorem 6.4 yields explicit certificate bounds for averaged matrix energies and barrier-type objectives along affine paths. Example 7.4 illustrates the quadratic-energy case, while Example 7.7 shows

how the same mechanism provides a conservative certificate for commuting log-determinant barriers arising in covariance design and related matrix-valued workflows [23]. These examples demonstrate that the framework extends naturally from scalar regional averages to structured matrix averages while preserving computational transparency. At the same time, the noncommuting extension remains explicitly conditional, as discussed in Section 6, and should be interpreted in that qualified sense.

Overall, the main implication is that the present framework converts generalized convexity assumptions into explicit and numerically checkable certificate formulas. Its contribution is therefore not to replace numerical solvers, but to provide analytically grounded bounds that can be embedded into broader computational workflows whenever auditable average-value estimates, conservative screening rules, or reusable kernel constants are required. In this sense, the theory provides a practical bridge between generalized inequality analysis and implementable certificate construction in computational and applied mathematics.

10. DISCUSSION AND LIMITATIONS

In the classical convex specialization, Hermite–Hadamard bounds are known to be sharp for a class of affine functions, as reported in [1, 6]. In the case of the modified notion of (h, m)-convexity considered in this paper, sharpness depends on a more complex interaction among h, m, s, and the coefficients $H_\alpha(h, s)$ and $\widetilde{H}_\alpha(h, s)$ involved in the derived bounds. The form of these constants indicates that sharpness may be affected not only by the convexity model but also by the weights involved in the kernel.

The box bounds of Section 4 are clear and easily auditable, but their direct computation requires 2^n vertex values. This is acceptable in low-dimensional spaces where vertex enumeration is computationally inexpensive, but it may become limiting in higher-dimensional settings. In such situations, these formulas should be viewed primarily as exact certificate representations that may guide the development of approximation algorithms requiring fewer vertex evaluations.

Another structural limitation arises from the geometric setting adopted in the analysis. The results are formulated for origin-anchored domains of the form $\prod_{i=1}^{n}[0, b_i]$, for which the feasibility condition $mD \subseteq D$ is particularly transparent. While translated boxes can be handled through affine coordinate transformations, extending the present certificates to more general convex polytopes would require additional geometric compatibility conditions between the domain and the modified mixing structure.

Finally, the operator-theoretic extension in Section 6 relies on the commuting matrix regime, where scalar inequalities can be lifted through simultaneous diagonalization [15]. Although this setting already covers several practical scenarios, including diagonal covariance models and frequency-wise decompositions, the development of broadly applicable non-commuting operator extensions remains challenging. In particular, establishing verifiable compatibility conditions for Loewner-order modified (h, m)–convexity in the presence of nonlinear operator weights is still an open analytical problem [18].

11. CONCLUSION AND FUTURE WORK

This paper develops a kernel-weighted framework of explicit vertex certificates for functions satisfying modified (h, m)–convexity of the second type. The main outcome is a family of computable bounds, including one-dimensional kernel-weighted estimates, dimension-explicit vertex certificates on boxes, radial bounds on origin-anchored simplices, and rigorous trace inequalities in the commuting matrix regime under functional calculus. In the noncommuting setting, the extension is stated deliberately in a conditional form under an operator-compatibility hypothesis, thereby keeping the operator-theoretic claims mathematically precise.

A central feature of the framework is that the resulting constants are explicit, one-dimensional, and numerically reusable. This makes the certificates directly verifiable and computationally accessible. The numerical investigations show that the kernel coefficients can be evaluated efficiently and that the resulting bounds can be checked independently through exact computation when available, quadrature-based approximation, and Monte Carlo validation. In this sense, the paper contributes to computational and applied mathematics by converting generalized convexity assumptions into numerically checkable certificate constructions.

The illustrative applications considered in this work, including quadratic losses, commuting matrix energies, economic-dispatch envelopes, RLC stored-energy bounds, and commuting log-determinant barriers, should be interpreted in this certificate-based sense. They demonstrate how the framework can support optimization-related and matrix-valued workflows through conservative average-value bounds, structured surrogate estimates, and reusable kernel constants. At the same time, these examples are not intended as full application-specific validation studies or stand-alone algorithmic developments. Their role is to show how the theory can be embedded into broader computational settings while preserving analytical transparency.

The framework also has clear limitations. On boxes, the certificate requires 2^n vertex evaluations, which makes

the present form most attractive in low and moderate dimensions. The multivariate development is formulated for origin-anchored boxes and simplices, whereas extensions to more general polyhedral geometries would require additional compatibility between the domain structure and the modified mixing rule. In the operator setting, the commuting regime remains the fully rigorous and computationally transparent case, while broadly applicable noncommuting extensions remain open.

Several directions for future work arise naturally. On the theoretical side, it would be valuable to derive sharper certificates, reduce the dependence on full vertex enumeration, extend the framework to wider geometric classes, and identify verifiable compatibility criteria in the noncommuting matrix setting. On the computational side, the present certificate machinery may be integrated into numerical workflows that require conservative regional-average bounds, auditable screening surrogates, or offline-online reuse of kernel constants across families of related instances. It would also be worthwhile to investigate how these certificates interact with adaptive quadrature, uncertainty quantification, and structured optimization pipelines in higher-dimensional settings. All numerical results reported in this paper are reproducible from the explicit formulas, parameter choices, quadrature descriptions, and sampling protocol given in Section 7.

REFERENCES

[1] Niculescu, Constantin, and Lars-Erik Persson. Convex Functions and Their Applications. Vol. 23. New York: Springer, 2006.

[2] Boyd, Stephen, and Lieven Vandenberghe. Convex Optimization. Cambridge university press, 2004.

[3] Ahmad, Muhammad Saeed, Aymen Flah, and Mujahid Abbas. "A Unified (v, w)-Strongly Convex Simpson-Type Framework for Non-Quadratic RLC Impedance Models in Energy Distribution Networks." IEEE Access 14 (2026): 18115-18137.

[4] Noor, Muhammad Aslam, and Khalida Inayat Noor. "Some new aspects of nonconvex inverse variational inequalities." Open Journal of Mathematical Sciences 9 (2025): 116-140.

[5] Polyak, Boris Teodorovich. "Existence theorems and convergence of minimizing sequences for extremal problems with constraints." Doklady Akademii Nauk. Vol. 166. No. 2. Russian Academy of Sciences, 1966.

[6] Dragomir, Sever S., and Charles Pearce. "Selected topics on Hermite-Hadamard inequalities and applications." Science direct working paper S1574-0358 (2003): 04.

[7] Ajmal, Muhammad, Ahmad, Muhammad Saeed, Rafaqat, Muhammad. Matrix-valued operator analysis in kernel-weighted multivariate modified (h, m)-convex optimization (2026). (Manuscript submitted for publication).

[8] Dragomir, Silvestru S. "On the Hadamard's inequlality for convex functions on the co-ordinates in a rectangle from the plane." Taiwanese Journal of Mathematics (2001): 775-788.

[9] Hwang, Dah-Yan, Kuei-Lin Tseng, and Gou-Sheng Yang. "Some Hadamard's inequalities for co-ordinated convex functions in a rectangle from the plane." Taiwanese journal of mathematics (2007): 63-73.

[10] Gao, Guilian, and Yong Zhong. "Some inequalities for Hausdorff operators." Mathematical Inequalities & Applications 17.3 (2014): 1061-1078.

[11] Ahmad, Muhammad Saeed, Aymen Flah, and Mujahid Abbas. "Improved Hermite-Hadamard bounds for (v, w)-strongly convex functions with applications to energy storage optimization." Results in Engineering (2025): 107999.

[12] Gómez, Lucas, Juan E. Nápoles Valdés, and J. Juan Rosales. "Hermite–Hadamard Framework for (h, m)-Convexity." Fractal and Fractional 9.10 (2025): 647.

[13] Rockafellar, R. Tyrrell. Convex Analysis. Vol. 28. Princeton university press, 1997.

[14] Jarad, Fahd, Thabet Abdeljawad, and Kamal Shah. "On the weighted fractional operators of a function with respect to another function." Fractals 28.08 (2020): 2040011.

[15] Bhatia, R. "Matrix Analysis, Springer." New York (1997).

[16] Bullen, Peter S. Handbook of Means and Their Inequalities. Vol. 560. Springer Science & Business Media, 2013.

[17] Chesneau, Christophe. "Unifying Hardy-Hilbert-type integral inequalities." Open Journal of Mathematical Sciences 9 (2025): 73-94.

[18] Hansen, Frank, and Gert Kjærgård Pedersen. "Jensen's inequality for operators and Löwner's theorem." Mathematische Annalen 258.3 (1982): 229-241.

[19] Kubo, Fumio, and Tsuyoshi Ando. "Means of positive linear operators." Mathematische Annalen 246.3 (1980): 205-224.

[20] Iqbal, Wasim, and A. U. Rehman. "Some refinements of Giaccardi and Petrovic's inequalities." Open Journal of Mathematical Sciences 9 (2025): 45-56.

[21] Van der Schaft, Arjan. L_2-Gain and Passivity Techniques in Nonlinear Control. Berlin, Heidelberg: Springer Berlin Heidelberg, 2000.

[22] Ajmal, Muhammad, Ahmad, Muhammad Saeed, Rafaqat, Muhammad. Kernel-based convex bounds for robust RLC impedance certification in energy distribution networks (2026). (Manuscript submitted for publication).

[23] Telatar, Emre. "Capacity of multi-antenna Gaussian channels." European Transactions on Telecommunications 10.6 (1999): 585-595.